Base-Catalyzed Peptide Hydrolysis Is Insensitive to Mechanical Stress

4 **AUTHORS**, INCLUDING:

Fei Xia
East China Normal University
31 PUBLICATIONS **211** CITATIONS

Frauke Gräter
Heidelberger Institut für Theoretische Studien
**100** PUBLICATIONS **2,668** CITATIONS

ARTICLE

Base-Catalyzed Peptide Hydrolysis Is Insensitive to Mechanical Stress

Fei Xia,[†,‡,§] Agnieszka K. Bronowska,[‡,§] Shanmei Cheng,[†] and Frauke Gräter*[,†,‡]

[†]CAS-MPG Partner Institute and Key Laboratory for Computational Biology (PICB), Shanghai 200031, P. R. China
[‡]Heidelberg Institutes for Theoretical Studies gGmbH, Schloss-Wolfsbrunnenweg 35, 69118 Heidelberg, Germany

S *Supporting Information*

ABSTRACT: Biochemical reactions can be guided by mechanical stress. An external force has been previously shown both experimentally and theoretically to act as a catalyst for the scission of a disulfide bond in thiol/disulfide exchange reactions. How the dynamics of peptide hydrolysis, one of the most prevalent biochemical reactions, is influenced by a stretching force was investigated here using combined quantum and molecular mechanical (QM/MM) simulations together with transition path sampling. Our simulations predict mechanical force to only marginally enhance the reactivity of the rate-limiting step, the nucleophilic attack of hydroxide to the peptide moiety, and not to alter the reaction mechanism, even though the peptide bond and its π-electron conjugation is weakened by force. We describe a previously unidentified hydrogen bonded intermediate state, which is likely to play a role in general in base-catalyzed and analogous enzymatic reactions. Our predictions can be directly tested by single molecule stretching experiments.
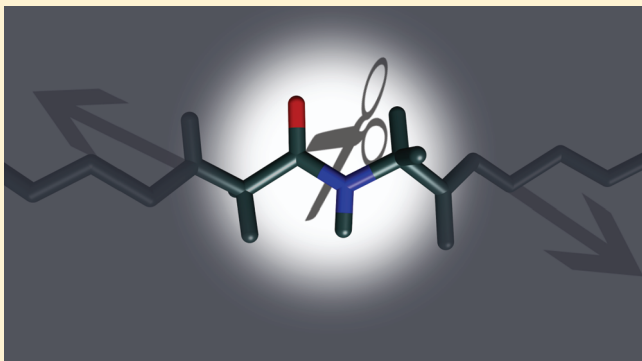
INTRODUCTION

Mechanical force not only crucially regulates the biological function of some mechanics-dependent proteins but also may similarly trigger the occurrence of specific biochemical reactions, among others those crucial for angiogenesis,[1] cell motility,[2] cell differentiation,[3] and hemostasis.[4] Recently, evidence has accumulated that some chemical reactions of physiological importance can be governed directly by mechanical force.[5,6] For instance, recent force-clamp AFM experiments have revealed that mechanical force accelerates the exchange reactions of disulfide bonds in proteins in case of chemical reducing agents.[7−9] The reaction rates measured in these experiments mainly followed an exponential dependency on the applied mechanical forces ranging from 100 pN up to 2000 pN, which could be explained on the basis of the simple Bell model.[10] Thus, mechanical force destabilizes the cleaving bond and promotes its scission. For enzymes as the reducing agent, however, opposite effects, i.e., slowing down the reaction rate with force, has also been observed in the low force regime.[11] Quantum chemical studies on these and other systems under force could give molecular insight into the force-induced acceleration of mechanochemical reactions by force.[12,13] We have previously successfully employed quantum and molecular mechanical (QM/MM) simulations combined with transition path sampling (TPS) to show that force can alter the free energy landscape underlying the disulfide bond exchange reaction along essential order parameters parallel as well as orthogonal to the direction of the applied force.[14] Force was found not only to increase the reaction rate by several orders of magnitude, in agreement with

experiments, but also to induce a shift in the transition state toward the reactant state. Taken together, the recent experimental and theoretical studies demonstrated that mechanical forces can serve as a mean to manipulate chemical reactions, importantly those of biological relevance.

One of the most frequent biochemical reactions is the hydrolysis of a peptide bond. Proteases are the most prevalent group of enzymes and serve as targets for many clinically relevant drugs.[15] While the catalytic mechanisms of various proteases are well-studied,[16] very little is known about the molecular mechanism under mechanical load. Many clinically relevant proteins such as phosphatases[17] and zinc metalloproteinases[18] operate under mechanical perturbations as they occur in the extracellular space such as stretching forces or the shear flow of blood.[19] Indeed, it has recently been shown that mechanical tension enhances the rate of proteolytic degradation in the extracellular matrix.[20] In this scenario, mechanical forces are passed onto individual protein domains, which subsequently (partially) unfold and potentially expose previously hidden proteolytic cleavage sites. Thus, the question arises if and how a stretching force acting on the protein backbone alters the rate and molecular mechanism of peptide bond cleavage catalyzed by these proteins. One example is ADAMTS13, a zinc metalloproteinase expressed in the plasma.[21] It cleaves the von Willebrand factor (VWF) A2 domain only under shear flow conditions, i.e., after mechanical unfolding,

supposedly involving stretching of the substrate around the cleavage site.[4] An impairment of this process leads to serious hematological conditions, such as thrombotic thrombocytopenic purpura (TTP) and certain types of von Willebrand disease,[22,23] or severe systemic inflammatory response.[24] Hence, to investigate the pathophysiological mechanism of these conditions, it is mandatory to investigate the peptide hydrolysis reaction under stretching forces acting on the cleaving peptide bond at atomic level.

Here, we study the nonenzymatic hydrolysis of a peptide under an external mechanical force, as the first step to investigate the mechanochemistry of enzymatic peptide hydrolysis. We chose to investigate the base-catalyzed mechanism of hydrolysis, as this has been shown to be analogous to the mechanism of most proteases, including serine, tyrosine, or metalloproteases.[25,26] As the mechanism that also dominates in water at pH 7, it has been explored for decades both experimentally[27−29] and theoretically.[30−33] The consensus of previous experimental and theoretical studies is that both the enzymatic and nonenzymatic base-catalyzed hydrolysis of a peptide bond is a consecutive series of reactions. In the first rate-limiting step, a hydroxide ion as a nucleophile attacks the carbonyl carbon of the peptide to form a tetrahedral intermediate, as confirmed experimentally.[29] In the enzymatic case, instead of the hydroxide, a nucleophilic amino acid side chain (e.g., in serine proteases) or a metal-activated water molecule (in metalloproteases) acts as attacking nucleophile. The enzymatic and nonenzymatic mechanisms overall share the subsequent steps of rapid proton transfers and scission of the peptide bond.

We here aim at predicting the impact of force on the rate and mechanism of the first rate-limiting step of the hydroxide-catalyzed peptide hydrolysis reaction. We employ combined QM/MM simulations and extensive conformational sampling of reactive transitions, which together have previously proven useful for the disulfide bond reduction.[14] Force weakens the peptide bond by decreasing the extent of its π-electronic conjugation. However, the resulting charge redistribution causes an acceleration of the nucleophilic attack by only a factor of 4 within the investigated large range of forces (50−2000 pN). Independent from the force, we find the transition state region previously predicted to be stabilized by an intermolecular hydrogen bond. Our results on the mechanically assisted nonenzymatic hydrolysis of the peptide bond in solution may be experimentally verified by the AFM force-clamp measurements.

■ METHODS

Simulation System. All QM/MM simulations have been carried out using the interface[34] between the Gromacs 3.3.1[35] and Gaussian 03[36] packages. As a general and simple model for a protein substrate, a tetraglycine with protected N- and C-termini (N-acetylated and C-amidated, termed ACE and NAC, respectively) was chosen. The peptide was immersed in a cubic box of TIP4P[37] water. As shown in Figure 1a, the tetraglycine was divided into a region treated quantum mechanically (QM), which contained the central scissile peptide bond and a region treated molecular mechanically (MM). The QM region consisted of 18 atoms total, or 20 atoms in case the catalytic hydroxide anion was also included in the simulations. The MM region comprised the remaining part of the peptide and all water molecules. The QM/MM boundary involved two carbon—carbon atoms, of which the QM carbons were saturated with link atoms.[38] The explicit water environment allowed us to consider
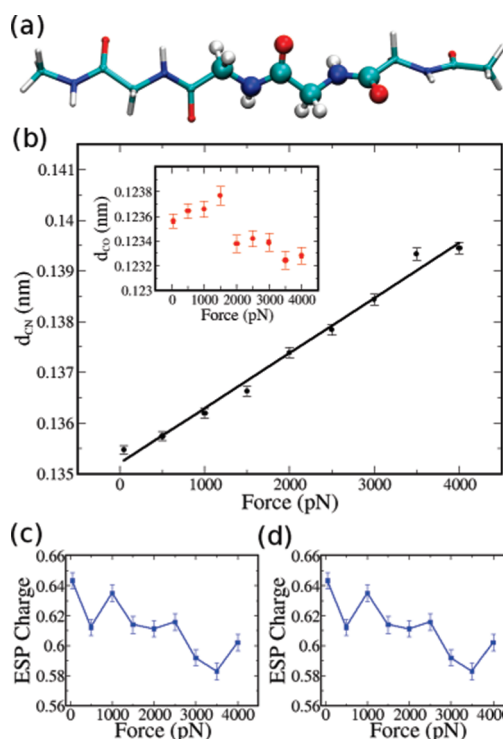

Figure 1. Peptide bond under a stretching force. (a) The tetraglycine model system, the reactant state RS of the nucleophilic attack considered here, is shown as sticks. Atoms treated quantum mechanically in the simulation are shown as spheres. The MM region includes the rest of the peptide and all water molecules. Two link atoms (not shown) were added at the interface of the QM and MM region to saturate the carbon atoms at the QM boundary. The external force was applied to the C_α atoms of two termini. (b) Average length of the C−N peptide bond, d_{CO}, shows a linear dependency on force. The inset shows the average length of the carbonyl bond, d_{CO}. (c), (d) Average partial (ESP) charge of the nitrogen (c) and carbon (d) atoms of the peptide bond at different forces.

direct solvation and stabilization of the hydroxide anion, which we find to essentially influence the reaction mechanism. Changes in protonation states, however, could not be taken into account, and the impact of force in this respect will be the subject of further investigations. The whole water box was neutralized by adding a sodium ion.

The QM region was treated with the DFT formalism, the hybrid functional B3LYP[39,40] combined with the 6-31G* basis set. The MM part was parametrized with the OPLS force field.[41] The cutoff for nonbonded interactions was 1 nm, the temperature was 300 K, and a constant pressure of 1 atm was applied. A Berendsen thermostat with a coupling constant of 0.1 ps, and a Berendsen barostat with a coupling constant of 1.0 ps was used.[42] The bonds involving the hydrogen atoms in the MM region were constrained using the LINCS[43] algorithm. The integration time step was 1 fs. Periodic boundary conditions were applied, and a cutoff value of 1 nm was used for long-range electrostatic interactions within the MM region. To handle the interactions between the QM and MM regions, the "normal" QM/MM scheme[44] was used.

Force-Clamp QM/MM Simultions. The systems, with and without a hydroxide ion, were initially treated fully molecular mechanically. Each system was energy-minimized with the steepest descent algorithm and then equilibrated in the NpT

10127

dx.doi.org/10.1021/jp202162r |*J. Phys. Chem. B* 2011, 115, 10126–10132

ensemble for 1 ns. It then was rotated by aligning the vector connecting the C_α atoms of ACE and NAC along the z-axis of the simulation box, and an external constant force was applied to these two C_α atoms. The system was then re-equilibrated for 1 ns under the external force. Several independent equilibrations were performed, with constant forces ranging from 50 to 4000 pN. Subsequent simulations were carried out with the hybrid QM/MM simulation, starting from the final structures equilibrated at the respective force. To setup up the system containing a hydroxide ion, the water molecule proximal to the central carbonyl carbon was replaced by the hydroxide anion by deleting one of the hydrogen atoms. Finally, the charge of the system was neutralized by adding one sodium cation, again by replacing a solvent molecule, which was chosen randomly.

Transition Path Sampling. To examine the ensemble of reactive pathways for the rate-limiting step of base-catalyzed peptide hydrolysis under force, we performed transition path sampling (TPS),[45−48] implemented in Gromacs. If not otherwise noted, we employed the same protocol and parameters previously applied to QM/MM simulations of the disulfide bond exchange reaction under force.[14] Shooting moves were performed by momentum displacements randomly chosen from a Gaussian distribution. We chose d_{CO}, the distance between the oxygen atom of the hydroxide anion and the peptide carbonyl atom, as the order parameter to define the reactant state (RS) and the product state, which here is the tetrahedral intermediate state (TIS) of the full hydrolysis reaction. Conformations with d_{CO} being larger than 0.30 nm were defined as the RS region, and with a distance d_{CO} smaller than 0.15 nm as RS. Any intermediate distance was regarded as the transition region. At five different forces, we generated a first reactive trajectory by restraining d_{CO} to 0.2 nm with a force constant of 20 kJ/mol/nm^2 in a QM/MM MD simulation at the respective constant force. This distance restraint caused the reaction to occur on the picosecond time scale. We harvested over 2000 trajectories for every force, with acceptance ratios of 34%, 32%, 37%, 38%, 39%, resulting in 772, 634, 754, 603, and 716 trajectories for forces of 50, 500, 1000, 1500, 2000 pN, respectively. Trajectories were largely decorrelated after <10 TPS cycles, ensuring sufficient sampling. From the ensemble of transition paths at each force, comprising up to six hundred trajectories per force with a constant length of 250 fs, we calculated rate constants as described previously.[14] To this end, we also performed additional transition path sampling in a series of windows spanning the order parameter from 0.1 to 0.5 nm. With a width of each window of 0.04 nm and an overlap of 0.02 nm, a fully continuous $C(t_0)$, the correlation function of state populations in time, was obtained. A time interval of $t_0 = 180$ fs was chosen for these simulations and the rate calculation. For theoretical details of the rate calculations, we refer to work by Bolhuis and coworkers.[48]

Natural Bond Orbital (NBO) Analysis. To check the robustness of the observed effect of force on RS and TIS with respect to the basis set, we additionally performed pure QM calculations using an extended basis set, namely B3LYP/6-31+G(d,p). These calculations were performed in vacuo using Gaussian03.[36] We fully optimized conformations sampled in the QM/MM MD simulations at each force in the presence of a distance constraint applied to the atoms serving as pulling groups in force-clamp simulations and calculated force-dependent bond lengths and partial charges for the optimized geometries (Supporting Information, Figure S1). The trends observed in QM/MM simulations were overall reproduced in these QM optimized structures, underlining the insensitivity of our results for the RS and TIS

electronic properties with regard to the basis set and solvation. We also performed natural bond orbital (NBO) analysis to quantify the force-induced weakening of the cleaving peptide bond.[49] NBOs are an orthonormal set of localized oligo-center orbitals, which describe the Lewis-like molecular bonding pattern of electron pairs in optimally compact form. Obtaining NBOs involves a gradual transformation of the nonorthogonal atomic orbitals into natural atomic orbitals, then into natural hybrid orbitals, and finally into natural bond orbitals. The mechanical strength of the peptide bond then was measured by the electronic population of its NBO. The closer the total population (POP) is to the maximal total population ($POP_{max} = 2$), the stronger the bond is. The total electronic population of a bond is the sum of the populations of bonding spin−orbitals, minus the sum of populations of antibonding spin−orbitals. Only those orbital interactions with energies higher than 0.25 kcal/mol were taken into account. For each C−N bond, only the major orbital−orbital interactions and no interactions involving lone pairs were considered in the analysis.

■ RESULTS

Peptide Bond under Force. To investigate the response of a peptide bond to mechanical stress, we carried out QM/MM equilibrium simulations of the peptide in water, in the absence and presence of a hydroxide anion. The tetraglycine moiety was equilibrated under forces between 50 and 4000 pN. The structural properties were calculated from the average of five independent trajectories at each force. Figure 1b shows the average length of the C−N bond in the QM region, d_{CN}, as a function of the external pulling force. The linear dependence on force indicates that the bond can be approximated as a harmonic oscillator within the sampled range of bond lengths.

The lengthening of the bond with force involves a slight but significant decrease in its electronic population by the orbital interactions involving the σ and σ^* orbitals, according to our natural bond orbital (NBO) analysis (Supporting Information, Figure S2). Mechanical force increasingly populates the σ^* orbital of the C−N bond, while it depopulates the σ orbital through its interaction with LUMO of the hydroxide anion. Thus, in the absence of mechanical forces, the conjugation of π electrons in the peptide moiety is known to result in a length and bond order of the C−N bond between a single and double bond, stretching forces interfere with the conjugation of the π electrons within the peptide bond, effectively decreasing its double bond character. As a result, the bond is weakened by mechanical force.

The increased localization of electrons involves higher negative charges on the nitrogen atom (Figure 1c). Simultaneously, mechanical force slightly reduces the positive charge on the carbon atom (Figure 1d), due to a donation of electron density from the carbonyl oxygen. The connecting C═O bond length does not show any drastic change (Figure 1b inset) but instead fluctuates by less than 0.01 nm over the range of forces. The elongation of the C−N bond, and the marginal changes in the C−O bond length by force, along with the tendencies observed for the carbon and nitrogen partial charges, were reproduced in quantum mechanical optimizations of the same system in vacuum (Supporting Information , Figure S1a−c). In summary, the C−N moiety elongates with force up to 4000 pN, and thereby undergoes an electron localization. The question arises whether this redistribution of electron density affects the reactivity for S_N2 hydrolysis by hydroxide. A probable scenario is that
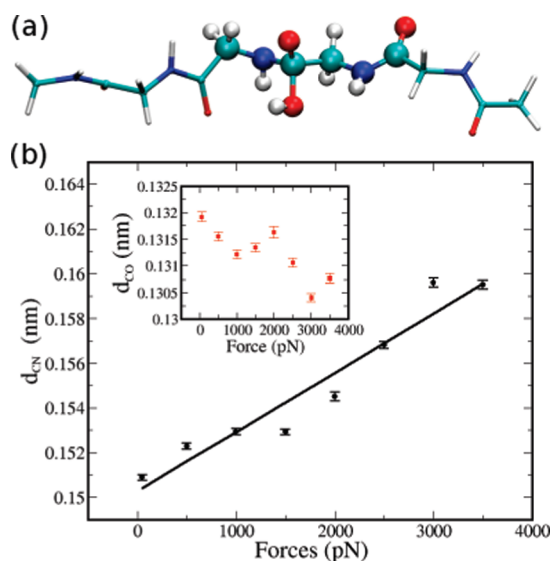
Figure 2. Tetrahedral intermediate state (TIS), the product of the reaction, under a stretching force. (a) TIS, depicted analogous to Figure 1a: spheres, QM region; stick, MM region. (b) Average length of the C—N peptide bond, d_{CO}, in the TIS. The inset shows the average length of the carbonyl bond, d_{CO}.

the weakening of the C—N bond for cleavage and the reduced positive charge on the attacked carbonyl have partly compensating effects, which we tested by transition path sampling (see below).

The product of the first half reaction of a base-catalyzed peptide hydrolysis as considered here is a tetrahedral intermediate state (TIS, Figure 2a). We compared the geometry and charge distribution of the TIS to the RS under varying forces (Figure 2b). Adding the hydroxide to the peptide elongates the C—N and C=O bonds by ~0.02 and 0.01 nm, respectively. Beyond 4000 pN, at which the bond reaches a length of nearly 0.16 nm, we observed C—N bond scission on a picosecond time scale. Thus, as expected, the attack of the hydroxide anion on the carbonyl carbon severely distorts the structure of the peptide bond. The conjugated C—N and C=O bonds evolve from double to single bonds upon formation of the new carbon-hydroxide bond.

Force-Dependent Dynamics of Nucleophilic Attack. To test if mechanical forces have an impact on the reactivity of the hydroxide nucleophilic attack, we performed transition path sampling at forces between 50 and 2000 pN. The hydroxide anion approached the peptide bond to form the TIS on a subpicosecond time scale (Figure 3a). Interestingly, at short distances of the hydroxide to the carbonyl group (d_{CO} < 0.25 nm), an intermediate state was observed, featuring a hydrogen bond between the hydroxide oxygen and the hydrogen of the adjacent NH group (d_{OH} = 0.17−0.18 nm; see snapshot in Figure 3a). The hydrogen bond again opens upon formation of the TIS, the product of the nucleophilic attack. The lifetime of the hydrogen bonded intermediate state (HBIS), as reflected by the plateau of d_{CO} (Figure 3a, black curve) is on the order of tens of femtoseconds. Previous theoretical studies of base-catalyzed peptide hydrolysis were based on formamide as the substrate.[30−33] While formamide successfully mimics a single peptide bond, it misses important features of a full peptide, including the hydrogen bond donor propensities of a neighboring peptide group as

identified here. Thus, to our knowledge for the first time, we here were able to describe a HBIS, which is likely to play a role in any base-catalyzed peptide hydrolysis reactions, as well as in related enzymatic reaction with an attacking nucleophile, such as matrix metalloproteinases. We tested the robustness of our findings by additional pure quantum mechanical optimizations, where we determined the HBIS and TS along d_{CO} at 50 pN. Even though a quantitative agreement cannot be expected between the explicit solvent QM/MM and the vacuum QM simulations with extended basis set, the QM calculations identified a HBIS exhibiting the same hydrogen bond with a distance of d_{OH} = 0.17 nm, though at shorter d_{CO} (0.17−0.18 nm).

We next analyzed the ensemble of trajectories at varying forces by projecting it onto the two major order parameters, the distance of the attacking hydroxide to the carbonyl group, d_{CO}, and the hydrogen bond distance of the intermediate, d_{OH} (Figure 3b−f). Except from slight variations in the population densities, no pronounced change in the reaction mechanism and the involved states with force is observed. The reaction hence proceeds largely independent from the external force. Also, the HBIS is detected throughout (d_{OH} = 0.15−0.2 nm), at a distance d_{CO} of 0.20−0.22 nm. Previous studies on formamide hydrolysis have reported transition regions with d_{CO} = 0.20−0.22 nm,[31] which coincides with the HBIS observed here. The hydrogen bond thus stabilizes the region of high energy structures and thereby can be expected to assist the formation of the TIS. We note that the region of the reaction product, the TIS, does not show a population maximum, because trajectories were stopped upon reaching the product reaching during the TPS. The other two maxima of the projected conformational density lie in the region of the RS, with d_{CO} = 0.5 and 0.4 nm, respectively. The barriers between these two minima and toward forming the HBIS are likely to be caused at least partly by the desolvation of the hydroxide anion, as we observed a decrease of hydrogen bonds of the nucleophile to surrounding water molecules in this region (Supporting Information, Figure S3).

Figure 3 does not show any pronounced shift of the transition path ensemble with the external stretching force, in sharp contrast to previous studies on disulfide bond reduction under varying force.[14] A slight shift of the HBIS to a longer hydrogen bond distance (0.22 nm) and thus to a decreased stabilization by the hydrogen bond, is found for the highest force of 2000 pN. Apparently, the force increasingly restricts the conformational space of the stretched peptide and thereby hampers hydrogen bond formation to the adjacent aminoacid. If this trends holds for forces larger than 2000 pN, further investigations are required. Similarly, the preferred attack angles of the hydroxide anion relative to the peptide bond are found to be insensitive with regard to the mechanical force (Supporting Information, Figure S4b,c). Independent of the mechanical force, at d_{CO} = 0.2 nm, the nucleophile and the carbonyl moiety form angles α_{COH} and α_{OCO} of 100−110°, in close agreement with the previously described geometries for this TS (each 107° [31,33]). Again, irrespective of the externally applied force, the angle formed between the hydroxide and the plane of the atoms N, C, and O of the peptide samples a range of 20−40° (Supporting Information, Figure S4d).

Rate Constants. Given the overall independence of the reaction mechanism from the external force, we would not expect any significant change in the reaction rates for this first step of the hydrolysis reaction. Indeed, the rate calculated from
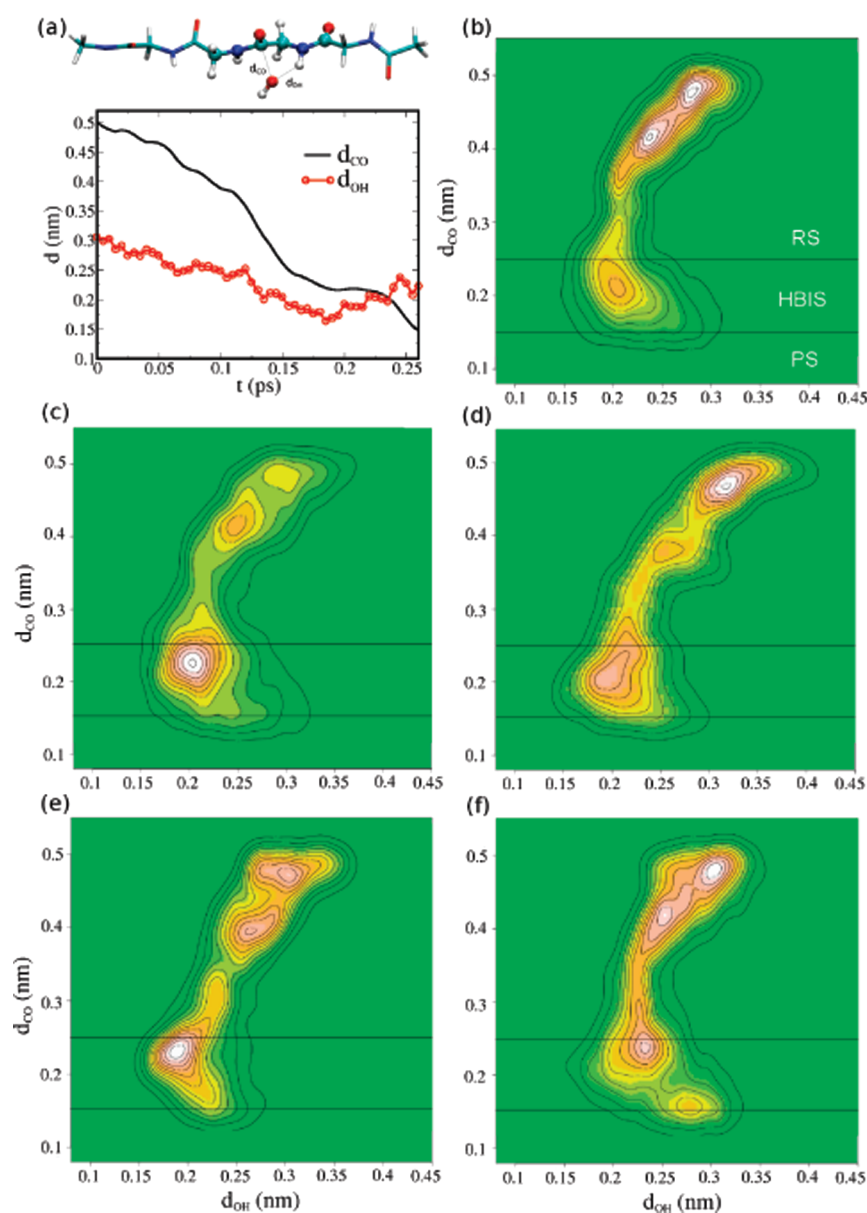
10129

dx.doi.org/10.1021/jp202162r |J. Phys. Chem. B 2011, 115, 10126–10132

Figure 3. Mechanism of nucleophilic attack features a hydrogen bonded intermediate (HBIS) and is not significantly altered by mechanical force. (a) A representative reactive trajectory obtained from TPS at 1500 pN is shown, projected onto d_{CO} (black) and the hydrogen bond distance d_{OH} (red). The distance measuring the progress of attack, d_{CO}, shows a plateau for short hydrogen bonds, reflecting the formation of the HBIS prior to the final formation of the product, the TIS. A structure of the HBIS is shown, with dashed lines indicating the two different order parameters, d_{rmCO} and d_{OH}. (b)−(f) Population densities as obtained from the ensemble of reactive trajectories obtained from TPS at forces between 50 and 2000 pN were projected onto the d_{CO} and d_{OH} distances. Solid lines indicate the borders of the reactant and product state regions. All projections feature highly similar RS and HBIS regions and transitions between them.

the transition path ensemble described above and additional shorter TPS trajectories (see Methods) increases by only a factor of ∼4 up to 1500 pN (Figure 4). This small acceleration corresponds to a change in the free energy barrier height be less than 2 kT and is significantly smaller than the acceleration that has been experimentally and theoretically observed for thiol/disulfide exchange reactions.[11,14] The relevant reaction coordinate for the first half-reaction of the hydrolysis, the attack of the hydroxide anion, is likely to be dominated by d_{CO}. This degree of freedom is largely orthogonal to the direction of the applied external force, which mainly acts along the peptide backbone, and thus along the C−N bond. On the other hand, force distributes

through this highly dimensional system also into degrees of freedom that are not parallel to the force vector. However, the resulting effects we observed, most importantly the increased electron localization and C−N bond weakening, apparently compensate each other such that the target for nucleophilic attack, the carbonyl carbon atom, remains largely unaffected from the pulling force. The result is an only marginal increase in reactivity up to 1500 pN. Interestingly, the rate again decreases from 1500 to 2000 pN, in line with the observation that the high force of 2000 pN interferes with the formation of the HBIS, and thus leads to an increase rather than a decrease in the free energy barrier of the reaction.
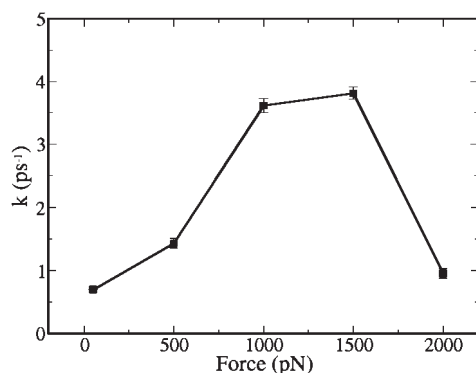
Figure 4. Rate constants of the S_N2 reaction, estimated from TPS at varying forces. They change no more than by a factor of 4 within the probed force regime.

CONCLUSION

We have demonstrated that the combination of QM/MM and TPS is a powerful tool for determining the nature of peptide bond scission under the influence of mechanical forces. We have previously validated this approach for the experimentally well-studied case of disulfide bond reduction in a peptide by dithiotriol under mechanical forces, where we observed a significant enhancement of reactivity and a shift in transition state with force,[14] in agreement with experiments. Here, the mechanical force is found to significantly alter the structural and electronic properties of the peptide by reducing electronic conjugation and weakening the C−N bond. The resulting increase in reactivity, however, is only found to be marginal as compared to the thiol/disulfide exchange reaction, the only other reaction for which force-dependent rates have been quantitatively determined in experiment and simulations. Also, the overall reaction mechanism is largely force-independent. The nucleophilic attack thus does not critically depend on the C−N bond strength, but rather on other degrees of freedoms orthogonal to and largely unaffected by the pulling force, such as the electron density in the carbonyl group of the peptide bond. Interestingly, the reactive trajectories revealed a stabilization of an intermediate by a hydrogen bond interaction of the hydroxide anion with the peptide backbone during the addition process. This hydrogen bonded intermediate, which to our knowledge has not been identified previously, might similarly play a decisive role in the peptide hydrolysis by enzymes like matrix metallo-proteinases.

We here focused on the first and rate-limiting step of base-catalyzed peptide hydrolysis, the formation of the TIS. The second step involves the scission of the C−N bond, which, as we could show, is weakened by force, and therefore might be cleaved at higher rates upon application of mechanical stress. It is plausible that for reactions catalyzed by other nucleophiles such as proteases, this second step might play the rate-limiting role, resulting in an overall increase in rate of the reaction by force.

Experiments on force-assisted peptide hydrolysis have not yet been accomplished. Monitoring the hydrolysis of single peptides under force clamp using atomic force microscopy could directly test our predictions from simulations. Candidates interesting to investigate in this respect are isopeptide bonds, which, being selectively strained within a folded protein, are appropriate substrates for selective and force-sensitive hydrolysis. In addition, apart from hydroxide anions as nucleophiles, i.e., high pH conditions, enzymatic catalysts promise to be an interesting

choice, given their selectivity for specific peptide bonds within proteins, and their versatile way of distributing and responding to mechanical force in terms of reactivity.[9,11] Further theoretical and experimental studies will have to test if our major finding that peptide hydrolysis is comparably insensitive toward a stretching force can be generalized to any hydrolysis reaction of a peptide bond, or if the sensitivity is enhanced for enzymatic reactions of this kind.

ASSOCIATED CONTENT

Ⓢ Supporting Information. Figures include bond lengths, partial charges, and the NBO analysis of the peptide bond, data on the solvation of the hydroxide anion, and hydroxide attack angles, all of which are shown as a function of force. This material is available free of charge via the Internet at http://pubs.acs.org.

AUTHOR INFORMATION

Corresponding Author
*E-mail: frauke.graeter@h-its.org.

Author Contributions
§These authors contributed equally.

ACKNOWLEDGMENT

REFERENCES

(1) Mammoto, A.; Mammoto, T.; Ingber, D. E. Rho signaling and mechanical control of vascular development. *Curr. Opin. Hematol.* **2008**, *15*, 228–234.

(2) Ghosh, K.; Thodeti, C. K.; Dudley, A. C.; Mammoto, A.; Klagsbrun, M.; Ingber, D. E. Tumor-derived endothelial cells exhibit aberrant Rho-mediated mechanosensing and abnormal angiogenesis in vitro. *Proc. Natl. Acad. Sci. U. S. A.* **2008**, *105*, 11305–11310.

(3) Li, B.; Li, F.; Puskar, K. M.; Wang, J. H. C. Spatial patterning of cell proliferation and differentiation depends on machanical stress magnitude. *J. Biomech.* **2009**, *42*, 1622–1627.

(4) Baldauf, C.; Schneppenheim, R.; Stacklies, W.; Obser, T.; Pieconka, A.; Schneppenheim, S.; Budde, U.; Gräter, F. Shear-induced unfolding activates von Willebrand factor A2 domain for proteolysis. *J. Thromb. Haemost.* **2009**, *7*, 2096–2105.

(5) Granick, S.; Bae, S. C. Physical chemistry: Stressed molecules break down. *Nature* **2006**, *440*, 738–743.

(6) Rosen, B. M.; Percec, V. Mechanochemistry: A reaction to stress. *Nature* **2007**, *446*, 381–382.

(7) Wiita, A. P.; Ainavarapu, S. R. K.; Huang, H. H.; Fernández, J. M. Force-dependent chemical kinetics of disulfide bond reduction observed with single-molecule techniques. *Proc. Natl. Acad. Sci. U. S. A.* **2006**, *103*, 7222–7227.

(8) Ainavarapu, S. R. K.; Wiita, A. P.; Dougan, L.; Uggerud, E.; Fernández, J. M. Single-molecule force spectroscopy measurements of bond elongation during a bimolecular reaction. *J. Am. Chem. Soc.* **2008**, *130*, 6479–6487.

(9) Garcia-Manyes, S.; Liang, J.; Szoszkiewicz, R.; Kuo, T. L.; Fernández, J. M. Force-activated reactivity switch in a bimolecular chemical reaction. *Nat. Chem.* **2009**, *1*, 236–242.

(10) Bell, G. I. Models for the specific adhesion of cells to cells. *Science* **1978**, *100*, 618–627.

10131

dx.doi.org/10.1021/jp202162r |*J. Phys. Chem. B* 2011, 115, 10126–10132

(11) Wiita, A. P.; Perez-Jimenez, R.; Walther, K. A.; Gräter, F.; Berne, B. J.; Holmgren, A.; Sanchez-Ruiz, J. M.; Fernández, J. M. Probing the chemistry of thioredoxin catalysis with force. *Nature* **2007**, *450*, 124–127.

(12) Ribas-Arino, J.; Shiga, M.; Marx, D. Understanding covalent mechanochemistry. *Angew. Chem., Int. Ed.* **2009**, *48*, 4190–4193.

(13) Hofbauer, F.; Frank, I. Disulfide bond cleavage: a redox reaction without electron transfer. *Chem.—Eur. J.* **2010**, *16*, 5097–5101.

(14) Li, W. J.; Gräter, F. Atomistic Evidence of How Force Dynamically Regulates Thiol/Disulfide Exchange. *J. Am. Chem. Soc.* **2010**, *132*, 16790–16795.

(15) Drag, M.; Salvesen, G. S. Emerging principles in protease-based drug discovery. *Nat. Rev. Drug Discov.* **2010**, *9*, 690–701.

(16) Topf, M.; Varnai, P.; Richards, W. G. Ab initio QM/MM dynamics simulation of the tetrahedral intermediate of serine proteases: Insights into the active site hydrogen-bonding network. *J. Am. Chem. Soc.* **2002**, *124*, 14780–14788.

(17) Grinthal, A.; Adamovic, I.; Weiner, B.; Karplus, M.; Kleckner, N. PR65, the HEAT-repeat scaffold of phosphatase PP2A, is an elastic connector that links force and catalysis. *Proc. Natl. Acad. Sci. U. S. A.* **2010**, *107*, 2467–2472.

(18) Lancellotti, S.; De Cristofaro, R. Structure and Proteolytic Properties of ADAMTS13, A Metalloprotease Involved in the Pathogenesis of Thrombotic Microangiopathies. *Prog. Mol. Biol. Transl. Sci.* **2011**, *99*, 105–144.

(19) Jin, S. Y.; Skipwith, C. G.; Zheng, X. L. Amino acid residues Arg(659), Arg(660), and Tyr(661) in the spacer domain of ADAMTS13 are critical for cleavage of von Willebrand factor. *Blood* **2010**, *115*, 2300–2310.

(20) Rajiv, J.; Susumu, S.; P. Harikrishnan, A.; Ascanio, D.; Arnab, M.; A. Philip, G.; Erzsebet, B.; Bela, S. Mechanical forces regulate elastase activity and binding site availability in lung elastin. *Biophys. J.* **2010**, *99*, 3076–3083.

(21) Sadler, J. E. A new name in thrombosis, ADAMTS13. *Proc. Natl. Acad. Sci. U. S. A.* **2002**, *99*, 11552–11554.

(22) Levy, G. G.; Motto, D. G.; Ginsburg, D. ADAMTS13 turns 3. *Blood* **2005**, *106*, 117.

(23) Rayes, J.; Hommais, A.; Legendre, P.; Tout, H.; Veyradier, A.; Obert, B.; Ribba, A. S.; Girma, J. P. Effect of von Willebrand disease type 2B and type 2M mutations on the susceptibility of von Willebrand factor to ADAMTS-13. *J. Thromb. Haemost.* **2007**, *5*, 321–328.

(24) Claus, R. A.; Bockmeyer, C. L.; Sossdorf, M.; Lösche, W. The balance between von-Willebrand factor and its cleaving protease ADAMTS13: biomarker in systemic inflammation and development of organ failure? *Curr. Mol. Med.* **2010**, *10*, 236–248.

(25) Grams, F.; Reinemer, P.; Powers, J. C.; Kleine, T.; Pieper, M.; Tschesche, H.; Huber, R.; Bode, W. X-ray structures of human neutrophil collagenase complexed with peptide hydroxamate and peptide thiol inhibitors implications for substrate-binding and rational drug design. *Eur. J. Biochem.* **1995**, *228*, 830–841.

(26) Tuchsen, E.; Woodward, C. Hydrogen-exchange kinetics of surface peptide amides in bovine pancreatic trypsin-inhibitor. *J. Mol. Biol.* **1987**, *193*, 793–802.

(27) Radzicka, A.; Wolfenden, R. Rates of uncatalyzed peptide bond hydrolysis in neutral solution and the transition state affinities of proteases. *J. Am. Chem. Soc.* **1996**, *118*, 6105–6109.

(28) Marlier, J. F.; Dopke, N. C.; Johnstone, K. R.; Wirdzig, T. J. A heavy-atom isotope effect study of the hydrolysis of formamide. *J. Am. Chem. Soc.* **1999**, *121*, 4356–4363.

(29) Ślebocka-Tilk, H.; Neverov, A. A.; Brown, R. S. Proton inventory study of the base-catalyzed hydrolysis of formamide. Consideration of the nucleophilic and general base mechanisms. *J. Am. Chem. Soc.* **2003**, *125*, 1851–1858.

(30) Bakoies, D.; Kollman, P. A. Theoretical study of base-catalyzed amide hydrolysis: gas- and aqueous-phase hydrolysis of formamide. *J. Am. Chem. Soc.* **1999**, *121*, 5712–5726.

(31) Cascella, M.; Raugei, S.; Carloni, P. Formamide hydrolysis investigated by multiple-steering ab initio molecular dynamics. *J. Phys. Chem. B* **2004**, *108*, 369–375.

(32) Gorb, L.; Asensio, A.; Tuñón, I.; Ruiz-López, M. F. The mechanism of formamide hydrolysis in water from ab initio calculations and simulations. *Chem.—Eur. J.* **2005**, *11*, 6743–6753.

(33) Blumberger, J.; Ensing, B.; Klein, M. L. Formamide hydrolysis in alkaline aqueous solution: insight from ab initio metadyanmics calculations. *Angew. Chem., Int. Ed.* **2006**, *45*, 2898–2897.

(34) Groenhof, G.; Bouxin-Cademartory, M.; Hess, B.; de Visser, S. P.; Berendsen, H. J. C.; Olivucci, M.; Mark, A. E.; Robb, M. A. Photoactivation of the photoactive yellow protein: why photon absorption triggers a trans-to-cis isomerization of the chromophore in the protein. *J. Am. Chem. Soc.* **2004**, *126*, 4228–4233.

(35) Lindahl, E.; Hess, B.; van der Spoel, D. Gromacs 3.0: A package for molecular simulation and trajectory analysis. *J. Mol. Model.* **2001**, *7*, 306–317.

(36) Frisch, M. J.; Trucks, G. W.; Schlegel, H. B.; Scuseria, G. E.; Robb, M. A.; Cheeseman, J. R.; Montgomery, J. A., Jr.; Vreven, T.; Kudin, K. N.; Burant, J. C.; et al. *Gaussian 03*, Revision C.02, Gaussian, Inc.: Wallingford, CT, 2004.

(37) Jorgensen, W. L.; Jenson, C. Temperature dependence of TIP3P, SPC, and TIP4P water from NPT Monte Carlo simulations: seeking temperatures of maximum density. *J. Comput. Chem.* **1998**, *19*, 1179–1186.

(38) Field, M. J.; Bash, P. A.; Karplus, M. A combined quantum-mechanical and molecular mechanical potential for molecular dynamics simulations. *J. Comput. Chem.* **1990**, *11*, 700–733.

(39) Becke, A. D. Density-Functional thermochemistry. 3. The role of exact exchange. *J. Chem. Phys.* **1993**, *99*, 3898–3905.

(40) Lee, C.; Yang, W.; Parr, R. G. Development of the colle-salvetti correlation-energy formula into a functional of the electron-density. *Phys. Rev. B* **1988**, *37*, 785–789.

(41) Jorgensen, W. L.; Chandrasekhar, J.; Madura, J. D.; Impey, R. W.; Klein, M. L. Comparison of simple potential functions for simulating liquid water. *J. Chem. Phys.* **1983**, *79*, 926–935.

(42) Berendsen, H. J. C.; Postma, J. P. M.; DiNola, A.; Haak, J. R. Molecular dynamics with coupling to an external bath. *J. Chem. Phys.* **1984**, *81*, 3684–3690.

(43) Hess, B.; Bekker, H.; Berendsen, H. J. C.; Fraaije, J. G. E. M. LINCS: A linear constraint solver for molecular simulations. *J. Comput. Chem.* **1997**, *18*, 1463–1472.

(44) Warshel, A.; Levitt, M. J. Theoretical studies of enzymic reactions: dielectric, electrostatic and steric stabilization of the carbonium ion in the reaction of lysozyme. *J. Mol. Biol.* **1976**, *103*, 227–249.

(45) Dellago, C.; Bolhuis, P. G.; Csajka, F. S.; Chandler, D. Transition path sampling and the calculation of rate constants. *J. Chem. Phys.* **1998**, *108*, 1964–1977.

(46) Bolhuis, P. G.; Dellago, C.; Chandler, D. Sampling ensembles of deterministic transition pathways. *Faraday Discus.* **1998**, *110*, 421–436.

(47) Dellago, C. P. G.; Bolhuis; Chandler, D. On the calculation of reaction rate constants in the transition path ensemble. *J. Chem. Phys.* **1999**, *110*, 6617–6625.

(48) Bolhuis, P. G.; Chandler, D.; Dellago, C.; Geissler, P. L. Transition path sampling: Throwing ropes over rough mountain passes, in the dark. *Annu. Rev. Phys. Chem.* **2002**, *53*, 291–318.

(49) Foster, J. P.; Weinyhold, F. Natural hybrid orbitals. *J. Chem. Phys.* **1980**, *102*, 7211–7218.